But the additional enhancement of the thermal stability expected due to the increased miscibility in IPN's synthesized under high pressure was not observed (Figures 22 and 23). In other words, the weight loss was independent of synthesis pressure.

Acknowledgment. This work was supported by the Korea Science and Engineering Foundation. We thank Dr. J. K. Yeo and C. M. Oh of Lucky Ltd. for their help in the electron microscopy work.

Registry No. (1,4-Butanediol)·(polytetramethylene glycol)·(trimethylolpropane)·(MDI) (copolymer), 39281-41-9; (divinylbenzene)·(styrene) (copolymer), 9003-70-7; (1,4-butanediol)·(MDI)·(polytetramethylene glycol) (copolymer), 9018-04-6; polystyrene (homopolymer), 9003-53-6.

References and Notes

(1) Manson, J. A.; Sperling, L. H. "Polymer Blends and Composites"; Plenum Press: New York, 1976.
(2) Sperling, L. H. "Interpenetrating Polymer Networks and Related Materials"; Plenum Press: New York, 1981.
(3) Klempner, D.; Frisch, K. C. "Polymer Alloys"; Plenum Press: New York, 1977.
(4) Kim, S. C.; Klempner, D.; Frisch, K. C.; Radigan, W.; Frisch, H. L. *Macromolecules* **1976**, *9*, 258.
(5) Lee, D. S.; Kim, S. C. *Macromolecules* **1984**, *17*, 2193.
(6) Lee, D. S.; Kim, S. C. *Macromolecules* **1984**, 17, 268.
(7) Lee, D. S.; Kim, S. C. *Macromolecules* **1984**, *17*, 2222.
(8) Bernstein, R. E.; Cruz, C. A.; Paul, D. R.; Barlow, J. W. *Macromolecules* **1977**, *10*, 681.
(9) Robard, A.; Patterson, D. *Macromolecules* **1977**, *10*, 1021.
(10) Patterson, D.; Robard, A. *Macromolecules* **1978**, *11*, 690.
(11) Kim, S. C.; Klempner, D.; Frisch, K. C.; Frisch, H. L. *Macromolecules* **1977**, *10*, 1187 and 1191.
(12) Nielsen, L. E. "Mechanical Properties of Polymers and Composites"; Marcel Dekker: New York, 1974; Vol. 2, 395.
(13) Dickie, R. A. *J. Appl. Polym. Sci.* **1973**, *17*, 45 and 2509.
(14) Dickie, R. A.; Cheung, M. F.; Newman, S. *J. Appl. Polym. Sci.* **1973**, *17*, 65.
(15) Dickie, R. A.; Cheung, M. F. *J. Appl. Polym. Sci.* **1973**, *17*, 79.
(16) Kerner, E. H. *Proc. Phys. Soc., London, Sect. B.* **1956**, *69*, 808.
(17) Budiansky, B. *J. Mech. Phys. Solids* **1965**, *13*, 223.
(18) Frisch, K. C.; Klempner, D.; Frisch, H. L. *Polym. Eng. Sci.* **1982**, *22*, 1143.
(19) Flory, P. J.; Rehner, J. *J. Chem. Phys.* **1943**, *11*, 512.
(20) Thiele, J. L.; Cohen, R. E. *Polym. Eng. Sci.* **1979**, *19*, 284.
(21) Siegfried, D. L.; Thomas, D. A.; Sperling, L. H. *Macromolecules* **1979**, *12*, 586.
(22) Tobolsky, A. V.; Shen, M. C. *J. Appl. Phys.* **1966**, *37*, 1952.
(23) Galanti, A. V.; Sperling, L. H. *Polym. Eng. Sci.* **1970**, *10*, 177.
(24) Bell, J. P. *J. Polym. Sci., Part A-2* **1970**, *6*, 417.
(25) Hargest, S. C.; Manson, J. A.; Sperling, L. H. *J. Appl. Polym. Sci.* **1980**, *25*, 469.
(26) Lipatov, Y. S.; Sergeeva, L. M.; Mozzhukhina, L. V.; Apukhtina, N. P. *Polym. Sci. USSR (Engl. Transl.)* **1974**, *16*, 2658.
(27) Kim, S. C.; Klempner, D.; Frisch, K. C.; Frisch, H. L. *J. Appl. Polym. Sci.* **1977**, *21*, 1289.

Study of Miscibility and Critical Phenomena of Deuterated Polystyrene and Hydrogenated Poly(vinyl methyl ether) by Small-Angle Neutron Scattering

Mitsuhiro Shibayama,† Hsinjin Yang, and Richard S. Stein*

Polymer Research Institute, University of Massachusetts, Amherst, Massachusetts 01003

Charles C. Han

National Bureau of Standards, Gaithersburg, Maryland 20899. *Received December 7, 1984*

ABSTRACT: Miscibility and critical phenomena were studied on the polymer system of deuterated polystyrene and hydrogenated poly(vinyl methyl ether) by the small-angle neutron scattering technique. The phase diagram was constructed with "light" and "neutron" cloud points as well as spinodal points. It shows a well-known behavior of a lower critical solution temperature. The agreement between the "light" and "neutron" cloud points is fairly good for all compositions. The correlation length, the statistical segment length, and the Flory–Huggins χ-parameter were obtained as functions of temperature and composition by employing de Gennes' scattering equation for polymer blends. The χ-parameter showed not only a temperature dependence but also a composition dependence. Comparison of the χ-parameter with the lattice fluid theory shows that the composition dependence of χ results from the lattice fluid nature of the system, i.e., the compressibility and the thermal expansion of the system.

I. Introduction

After the discovery of miscible polymer blends,[1] their study has been of great interest. The miscibility has usually been discussed in terms of the Flory–Huggins interaction parameter χ or the second virial coefficient A_2. In these studies, small-angle neutron scattering (SANS) is one of the most powerful methods for obtaining the χ-parameter because of the high contrast between labeled and unlabeled species. Zimm analyses have usually been done making the analogy of polymer–solvent systems,[2] which is only valid for dilute systems. Recently, the theory has been extended to apply to concentrated polymer–polymer mixtures,[3-7] where the concentration dependence of the χ-parameter became apparent.[8,9] Prior to SANS experiments, the concentration dependence of the χ-parameter had been observed by 1950.[10] Koningsveld et al. used this concentration dependence to explain their light scattering experiment results in polymer–solvent systems[11] and later polymer–polymer systems.[12] Although the existence of the lower critical solution temperature (LCST) was explained by introducing the equation of state theory[13,14] and the lattice fluid theory,[15,16] the concentration dependence of the χ-parameter has not been well understood. The correlation length is also a measure of the miscibility and plays an important role in the vicinity of the critical point.

We have reported a novel method for obtaining the cloud point in a polymer blend by SANS,[17] the "neutron"

† Present address: Department of Polymer Science and Engineering, Faculty of Textile Science, Kyoto Institute of Technology, Matsugasaki, Sakyo-ku, Kyoto, 606 Japan.

0024-9297/85/2218-2179$01.50/0

cloud point, which might be particularly useful for the isotopically labeled systems.

In this paper we first construct the phase diagram for deuterated polystyrene and hydrogenated poly(vinyl methyl ether) in terms of the "neutron" cloud point method as well as the conventional "light" cloud point, and we explore the reversibility of the phase separation and the phase annihilation by the neutron cloud point measurements. The spinodal points are also observed as a function of composition by the correlation length approach.[17,18] Second, we explore the critical concentration fluctuations by means of the temperature dependence of the correlation length and the susceptibility (the Rayleigh ratio at zero angle). Third, the average statistical segment length that is affected by the polydispersity of the components[19] is discussed as a function of temperature and composition. Finally, the concentration dependence of the experimental (or apparent) χ-parameter is compared to the lattice fluid model.

II. Theory

For describing the concentration fluctuation in the reciprocal space, it is convenient to use the Rayleigh factor $\mathcal{R}(q,T)$ at a scattering vector q and temperature T, which is identical with the differential scattering cross section $(\partial\Sigma/\partial\Omega)$,

$$\mathcal{R}(q,T) = \frac{I(q,T)}{I_0 V_{ir}} p^2 \tag{1}$$

$$q = (4\pi/\lambda) \sin(\theta/2) \tag{2}$$

where the $I(q,T)$ is the scattered intensity at q and T. I_0, p, and V_{ir} are the incident beam intensity, the sample-to-detector distance, and the irradiated volume, respectively. λ and θ are respectively the wavelength of the neutron and the scattering angle. In the case of two-component systems, the Rayleigh factor $\mathcal{R}_c(q,T)$ due to the concentration fluctuation is related to the osmotic compressibility of the system and given by the Einstein fluctuation theory[20]

$$\mathcal{R}_c(q = 0, T) = K\frac{RTC_B}{(\partial\Pi_A/\partial C_B)_T} \tag{3}$$

$$\mathcal{R}_c(q = 0, T) = KRTC_B^2\kappa_\Pi \tag{4}$$

where K and R are constants that depend on the nature of radiation used and the gas constant. κ_Π is the osmotic compressibility and defined as follows:

$$\kappa_\Pi = \frac{1}{C_B}\left(\frac{\partial\Pi_A}{\partial C_B}\right)^{-1} \tag{5}$$

where C_B and Π_A are the concentration of the B component in g/cm^3 and the osmotic pressure of the A component, respectively. At the critical point κ_Π becomes infinite and $\mathcal{R}_c(q,T)$ does also. We assume that the contribution of the concentration fluctuations can be extracted from the observed Rayleigh factor $\mathcal{R}_{obsd}(q,T)$, which consists of the density fluctuations, $\mathcal{R}_i(q,T)$, as well as the concentration fluctuation

$$\mathcal{R}_c(q,T) = \mathcal{R}_{obsd}(q,T) - [\phi_A\mathcal{R}_A(q,T) + \phi_B\mathcal{R}_B(q,T)] \tag{6}$$

where $\mathcal{R}_i(q,T)$ is the Rayleigh factor for pure component i with volume fraction of ϕ_i.

In the case of neutron scattering, K is given by[4]

$$K = (N/m_B{}^{*2})(a_A{}^* - a_B{}^*)^2 \tag{7}$$

where N is Avogadro's number, and $a_i{}^*$ and $m_i{}^*$ are the reduced scattering length and the reduced molecular weight per segment of component i and are given by

$$a_i{}^* = (v_0/v_i)a_i \tag{8}$$

$$m_i{}^* = (v_0/v_i)m_i \tag{9}$$

a_i and m_i being the scattering length per mole of monomer of i and the monomer molecular weight of i, respectively. v_0 and v_i are respectively the molar volume of the reference unit cell and of segments of i. K is dependent on the choice of the reference component. Therefore, we often use another constant defined as

$$k_N = N\left(\frac{a_A}{v_A} - \frac{a_B}{v_B}\right)^2 = \frac{m_B{}^{*2}}{v_0{}^2}K \tag{10}$$

which is independent of the choice of the reference volume.

Dilute Limit. In the limit of dilute solution, Π_A is described by[21]

$$\Pi_A = RT[(C_B/M_B) + A_2C_B{}^2 + ...] \tag{11}$$

and therefore we obtain the well-known Zimm equation

$$KC_B/\mathcal{R}_c(0,T) = (1/M_B) + 2A_2(T)C_B \tag{12}$$

where M_i is the molecular weight of i and $A_2(T)$ is the second virial coefficient, which can be described by the mass density ρ_i and the reduced polymerization index y_i as follows:

$$A_2 = \frac{1/2 - y_A\chi}{\rho_B{}^2 y_A v_0} \tag{13}$$

where χ is the Flory–Huggins interaction parameter. y_i is defined by

$$y_i = (v_i/v_0)z_i \tag{14}$$

where z_i is the polymerization index of the component i.

Concentrated Mixture. In the case of a concentrated mixture we cannot start with eq 11 because it neglects the higher terms of the virial expansion with respect to C_B. Three approaches to the description for the scattering function from polymer blends are now available, i.e., the modified Zimm equation,[4] the de Gennes scattering function,[3,5] and the extended Ornstein–Zernike theory,[6,7] and they are identical in some respects. We will review them in the Appendix and only describe the final results in the following sections.

Modified Zimm Equation. Stein et al.[4] extended the Zimm equation (eq 12) in terms of the Flory–Huggins theory. The free energy of mixing per unit volume is given by

$$\Delta G = \frac{RT}{v_0}\left[\frac{\phi_A}{y_A}\ln\phi_A + \frac{\phi_B}{y_B}\ln\phi_B + \chi\phi_A\phi_B\right] \tag{15}$$

The scattering factor can be expressed (see Appendix) as

$$\frac{Km_B{}^{*2}}{\mathcal{R}_c(0,T)v_0} = \frac{1}{y_A\phi_A} + \frac{1}{y_B\phi_B} - 2\chi \tag{16}$$

or

$$\left\{\frac{K}{\mathcal{R}_c(0,T)} - \frac{C_B}{v_0 y_A \rho_B{}^3[1 - C_B/\rho_B]}\right\}C_B = \frac{1}{M_B} + 2A_2C_B \tag{17}$$

Equations 16 and 17 allow us to estimate the χ-parameter for any composition.

de Gennes' Scattering Function. de Gennes[3] derived a scattering function for polymer blends based on the random phase approximation. Higgins et al.[5] extended this technique to the two-component system in which one component is a mixture of deuterated and hydrogenated

polymers. Higgins et al. have also removed the restriction of the equal segmental volume assumption.

By following de Gennes approach (see Appendix) for polymer blends with a mean field type of potential U between the A and B kind of monomers at a given volume fraction ϕ, the scattering Rayleight factor can be obtained as

$$\frac{1}{\mathcal{R}_c(q,T)}k_N = \frac{1}{v_A z_A \phi_A g_D(u_A)} + \frac{1}{v_B z_B \phi_B g_D(u_B)} - \frac{2Uv_0}{v_A v_B} \tag{18}$$

If we make an identification with eq A-4 at $q \to 0$, then eq 18 becomes

$$\frac{1}{\mathcal{R}_c(q,T)}k_N = \frac{1}{v_A z_A \phi_A g_D(u_A)} + \frac{1}{v_B z_B \phi_B g_D(u_B)} - \frac{2\chi}{v_0} \tag{19}$$

where we used the relation[22]

$$U = v_A v_B \chi / {v_0}^2$$

It should be pointed out that the first and second derivatives of χ with respect to ϕ were assumed to be negligible relative to χ in eq A-4. However, this assumption is not necessary in this approach. All we have to assume is that the random-phase approximation is valid at all compositions and that a mean field potential U, which may be a function of ϕ, can still be found for that composition. In other words, the parameter U or χ we used here includes the contributions from $\partial\chi/\partial\phi$ and $\partial^2\chi/\partial\phi^2$ terms. Therefore, this is not strictly identical with the original definition of the Flory–Huggins χ-parameter, which is pure enthalpic. Equation 19 is the central result of this section and is identical with eq 16 and the modified Zimm equation (eq 17) obtained from Flory–Huggins theory when $q = 0$. When q is small, e.g., $u_i < 1$, one can rewrite eq 19 as

$$\frac{1}{\mathcal{R}_c(q,T)}k_N = \left[\frac{1}{v_A z_A \phi_A} + \frac{1}{v_B z_B \phi_B} - \frac{2\chi}{v_0}\right] + \frac{1}{18\phi_A\phi_B}\left[\phi_A\phi_B\left(\frac{{b_A}^2}{v_A\phi_A} + \frac{{b_B}^2}{v_B\phi_B}\right)\right]q^2 = \frac{2}{v_0}(\chi_S - \chi) + \frac{1}{18\phi_A\phi_B}\frac{\overline{b^2}}{v_0}q^2 \tag{20}$$

$$\frac{\overline{b^2}}{v_0} = \phi_A\phi_B\left(\frac{{b_A}^2}{v_A\phi_A} + \frac{{b_B}^2}{v_B\phi_B}\right) \tag{21}$$

The polydispersity effect was first considered in the polymer–solvent system by Brinkman and Hermans[23] and later applied to the polymer–polymer case by Joanny,[19] and eq 20 is modified as

$$\frac{1}{\mathcal{R}_c(q,T)}k_N = \left[\frac{1}{v_A\langle z_A\rangle_w\phi_A} + \frac{1}{v_B\langle z_B\rangle_w\phi_B} - \frac{2\chi}{v_0}\right] + \frac{1}{18\phi_A\phi_B}\left[\phi_A\phi_B\left(\frac{\langle z_A\rangle_z {b_A}^2}{\langle z_A\rangle_w v_A\phi_A} + \frac{\langle z_B\rangle_z {b_B}^2}{\langle z_B\rangle_w v_B\phi_B}\right)\right]q^2 = \frac{2}{v_0}(\chi_s - \chi) + \frac{1}{18\phi_A\phi_B}\frac{b^2}{v_0}q^2 \tag{22}$$

$$\frac{\chi_s}{v_0} = \frac{1}{2}\left[\frac{1}{v_A\langle z_A\rangle_w\phi_A} + \frac{1}{v_B\langle z_B\rangle_w\phi_B}\right] \tag{23}$$

$$\frac{\overline{b^2}}{v_0} = \left[\phi_A\phi_B\left(\frac{\langle z_A\rangle_z}{\langle z_A\rangle_w}\frac{{b_A}^2}{v_A\phi_A} + \frac{\langle z_B\rangle_z}{\langle z_B\rangle_w}\frac{{b_B}^2}{v_B\phi_B}\right)\right] \tag{24}$$

Table I
Material Characteristics

code	mol wt M_w	mol wt M_n	mol wt M_z	polydispersity M_w/M_n	polydispersity M_z/M_w	density, g/cm³
PSD	255 000	230 000	270 000	1.11	1.06	1.116
PVME	99 000	46 500	170 000	2.13	1.72	1.047

Table II
Sample Characteristics

code	wt % PSD	ϕ_{PSD}	$\chi_s/v_0 \times 10^5$, mol/cm³
D10	10	0.0944	2.902
D20	20	0.1900	1.804
D25	25	0.2382	1.613
D30	30	0.2868	1.504
D40	40	0.3848	1.428
D50	50	0.4840	1.477
D60	60	0.5846	1.647
D80	80	0.7896	2.790

where $\langle z_i\rangle_w$ and $\langle z_i\rangle_z$ are the weight and the z-average polymerization indices.

In the following sections the polydispersity effect will be taken into account, particularly for the estimation of χ_S/v_0 and $\overline{b^2}/v_0$. Equation 20 or 22 can be written in the Ornstein–Zernike form for small q

$$\mathcal{R}_c(q,T) = \mathcal{R}_c(0,T)/(1 + \xi^2(T,\phi)q^2) \tag{25}$$

$$\mathcal{R}_c^{-1}(0,T) = (2/v_0)[\chi_s - \chi] \tag{26}$$

$$\xi^2(T,\phi) = \frac{\overline{b^2}}{36}[\phi_A\phi_B(\chi_s - \chi)]^{-1} = \frac{\overline{b^2}/v_0}{36}\left[\phi_A\phi_B\left(\frac{\chi_s}{v_0} - \frac{\chi}{v_0}\right)\right]^{-1} \tag{27}$$

where $\xi(T,\phi)$ is the correlation length at temperature T and at composition $\phi = \phi_A$.

In the vicinity of the phase separation temperature, $\mathcal{R}_c(0,T)$ and $\xi(T,\phi)$ may have scale forms as often observed in critical fluctuation phenomena[24]

$$\mathcal{R}_c(0,T) = \mathcal{R}_{c0}\epsilon^{-\gamma} \tag{28}$$

$$\xi(T,\phi) = \xi_0(\phi)\epsilon^{-\nu} \tag{29}$$

where

$$\epsilon = |(T - T_{sp})/T_{sp}| \tag{30}$$

where T_{sp} is the spinodal temperature.

III. Experimental Section

Materials. Deuterated polystyrene (PSD) and hydrogenated poly(vinyl methyl ether) (PVME) were obtained from Polymer Laboratories,[32] Stow, OH, and Scientific Polymer Products, Webster, NY, respectively. The characteristics are listed in Table I. The molecular weights were obtained by GPC. The poly(vinyl methyl ether) was kept under vacuum before use to avoid moisture. The mass density ρ was obtained in terms of the density gradient tube method at room temperature.

Sample Preparation. The prescribed components were dissolved in toluene and then cast into films. After being dried under vacuum at 70 °C for a week and then at 110 °C for a day, the films were compression-molded at 80–110 °C into disks of 19-mm diameter and 1.7-mm thickness and then mounted in a brass cell covered with 0.025-mm-thick copper shims. Samples were coded based on the weight percentage of PSD; e.g., D10 is PSD/PVME 10/90 wt %. Table II shows the list of the samples with the volume fraction of PSD (ϕ_{PSD}) as well as with χ_s/v_0 obtained from eq 23.

Small-Angle Neutron Scattering Experiments. Both the temperature-scanning SANS and the static measurements were conducted with the SANS facility at the National Bureau of

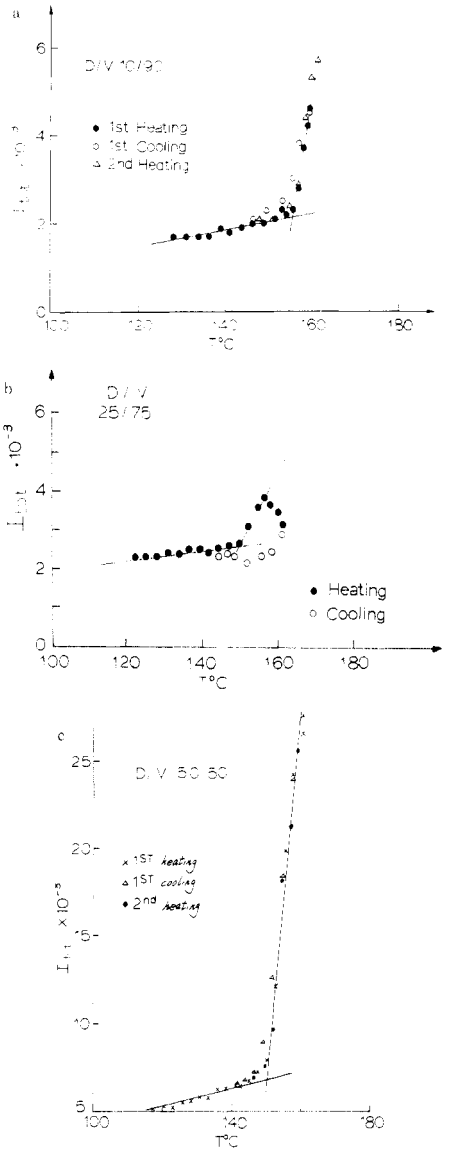

Figure 1. Neutron cloud point measurement curves, the total integrated intensity I_{tot} as a function of temperature for D10 (a), D25 (b), and D50 (c). The crossover of the straight lines shows the neutron cloud point.

Standards, Gaithersburg, MD. The wavelength, λ, of the incident beam was monochromatized to 6 Å by a velocity selector.

Temperature-Scanning Measurements. The sample was heated at a rate of 1 °C/min with a temperature programmer, Valley Forge Instrument Co. Inc., coupled with a copper heating block. Temperature was calibrated in terms of a Pt resistor. The scattered intensity was collected over the two-dimensional detector pixels ($0.005 < q < 0.12$ Å^{-1}), and the intensity due to electronic noise and room background was subtracted.

Static Measurements. The observed scattered intensity at a given temperature was circularly averaged and was corrected for oblique incidence, fast neutrons, and detector inhomogeneity. The absolute intensity calibration was done with dry silica gel as a secondary standard, which was calibrated in terms of a vanadium standard.[25] The relative error was within ±5%.

IV. Results and Discussion

Neutron Cloud Point. Figure 1 shows typical changes of the total integrated intensity I_{tot} with temperature obtained by the temperature-scanning SANS experiment. From the upturn of I_{tot} was determined the neutron cloud point T_{cp}^{N}. The hysteresis of I_{tot} with temperature was also examined. In the case of D25, which is about the critical composition, I_{tot} was not reversible. Contrary to this, D10 and D50 showed reversibility: each heating and cooling process has the same response in I_{tot}. The difference between the heating and cooling paths might be due to the time lag of the heat transfer between the sample and the heat bath. Only D20, D25, and D30, which are close to or on the critical composition, showed irreversible behavior. The physical meaning of I_{tot} is discussed in a previous paper.[17] The different behavior suggests that the phase separation occurs in a different manner: In the case of the critical composition (i.e., D25) phase separation occurs by spinodal decomposition, which allows a rapid domain growth from the range of SANS to that of light scattering in more or less a few minutes.[26] Well-developed domains have insufficient time to melt to the homogeneous mixture during the cooling process. On the other hand, in the case of the composition far away from the critical composition (e.g., D10 and D50), phase separation occurs by the nucleation and growth mechanism, whose kinetics are rather slow compared with that of spinodal decomposition.[27] Therefore, in the latter system, domains do not grow too much in a given time, thus easily melting to the original homogeneous mixture by cooling. Although similar hysteresis was observed by Nishi et al.[28] by the turbidity measurement with visible light, the interpretation of the reversibility requires further studies.

Table III
Characteristic Temperatures for PSD/PVME Blends

code	ϕ_{PSD}	cloud point T_{cp}^{L}, °C	cloud point T_{cp}^{N}, °C	T_{sp}, °C
D10	0.0944	154 ± 1	155.7	160.6
D20	0.1900	152 ± 1	151.5	154.3
D25	0.2382		150.0	153.4
D30	0.2868	151 ± 1	150.5	150.0
D40	0.3848		152.5	158.3
D50	0.4840	161 ± 1	156.0	160.7
D60	0.5846	161 ± 1	159.0	166.0
D80	0.7896	169 ± 1	168.5	177.7

It should be noted that even a well phase-separated sample could be transformed back to the original homogeneous mixture by annealing at a temperature below the phase separation temperature for about half a day. The annealed sample gave exactly the same neutron cloud point as that of the virgin sample. Although this result seems in conflict with that of Reich et al.[29] by light scattering and optical microscopy, it is probably due to the time scale of annealing and the sample dimensions, particularly the difference of the thickness.

The neutron cloud points were carefully compared with the conventional "light" cloud point T_{cp}^{L},[17] listed in Table III and shown in Figure 6 as well as the spinodal points. The agreement between the two kinds of cloud points was fairly good although it might be expected that there is a significant difference between the two cloud points due to the kinetic effect on the cloud-point measurement. Because it could take time for domains or concentration fluctuation to grow from the SANS range to the light scattering range, the cloud point could depend on the heating rate.

It is worthwhile to note that the cloud point is very sensitive to moisture as well as to the residual solvent. We observed more than ten degrees of depression of T_{cp}^{N} due mainly to moisture in our particular PS/PVME system.

Correlation Length Approach. Figure 2 shows the Rayleigh factor of D50 at different temperatures as a function of q, in which the Rayleigh factor increases markedly in the low-q regime with temperature. Employing the Ornstein–Zernike–Debye assumption (OZD) (eq 25), one can obtain a linear $1/\mathcal{R}_c(q,T)$ vs. q^2 relation-

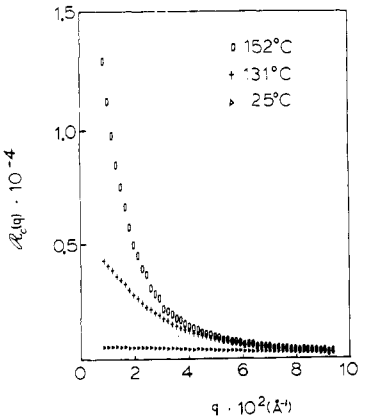

Figure 2. Variation of the scattered intensity profile with temperature for D50.

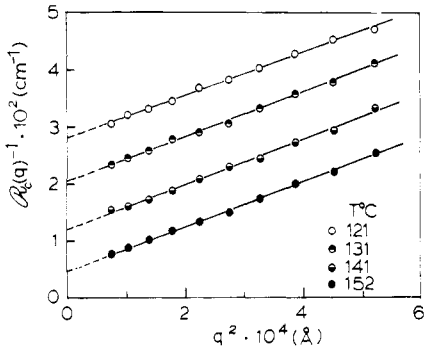

Figure 3. Reciprocal Rayleigh factor vs. q^2 plots (OZD plot) for D50 at various temperatures.

ship, as shown in Figure 3, the Rayleigh factor at zero angle $\mathcal{R}_c(q = 0,T)$ and the correlation length ξ. The experimental q range ($q > 0.007$ Å), however, was not small enough to apply the Ornstein–Zernike–Debye equation ($q < 0.007$ Å) because q must be smaller than $1/R_{gi}$, where R_{gi} is again the radius of gyration of the ith component. Therefore, we modified our analysis to remove the error due to the mismatching of the q range between the OZD assumption and this experiment.

Equation 19 can be written as

$$\frac{k_N}{\mathcal{R}_c(q,T)} \cong H\left(q,\frac{\chi}{v_0},\frac{\overline{b^2}}{v_0}\right) \tag{31}$$

where

$$H\left(q,\frac{\chi}{v_0},\frac{\overline{b^2}}{v_0}\right) = \frac{1}{v_A z_A \phi_A g_D(u_A')} + \frac{1}{v_B z_B \phi_B g_D(u_B')} - \frac{2\chi}{v_0} \tag{32}$$

$$u_i' = \frac{z_i v_i}{6}\left(\frac{\overline{b_i^2}}{v_0}\right)q^2 \tag{33}$$

By conducting a nonlinear regression on eq 31 with respect to χ/v_0 and $\overline{b^2}/v_0$, we obtained the solution $(\chi/v_0, \overline{b^2}/v_0)$. Then $\mathcal{R}_c(0,T)$ and $\xi(T)$ can be obtained from eq 16 and 27. It is impossible to estimate χ and $\overline{b^2}$ without v_0 because v_0 is a necessary lattice volume to give correct dimensionality. As we can see in eq 32 and 33, experiments give only the ratio χ/v_0 and $\overline{b^2}/v_0$, which are invariant with respect to v_0. Figure 4 shows an example of the linear and nonlinear regression on the reciprocal Rayleigh factor $1/\mathcal{R}_c(q,T)$ as a function of q^2 based on the OZD equation and the de Gennes equation, respectively. The circles show

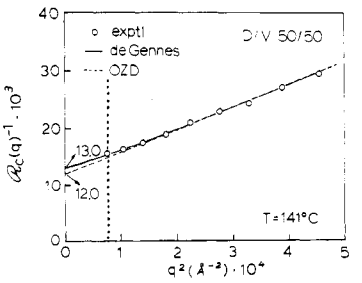

Figure 4. Comparison of the two analyses, OZD equation and de Gennes equation in the reciprocal Rayleigh factor vs. q^2 plot. The solid and dashed line denote the fitted lines based on de Gennes' equation and the OZD equation, respectively. The open circle shows the experimental point. The dotted line shows the upper limit of the OZD assumption.

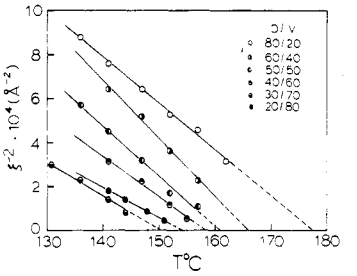

Figure 5. Reciprocal ξ^2 plot vs. temperature for various compositions. The intercept on the T axis gives the spinodal temperature.

Table IV
Comparison of the Characteristic Parameters $\mathcal{R}_c(q = 0,T)$ and $\xi(T)$ Obtained from the Two Different Approaches for D50

T, °C	$\mathcal{R}_c(q = 0,T)$, cm^{-1}		$\xi(T)$, Å	
	OZD	de Gennes	OZD	de Gennes
25	5.69	5.94	13.7	13.0
71	11.09	11.38	26.8	18.0
121	35.59	34.51	36.5	31.4
131	48.75	46.95	43.6	36.6
136	64.11	61.29	50.6	41.8
141	83.33	77.07	57.4	46.9
147	119.1	108.79	68.2	55.7
152	210.3	205.10	90.6	76.5
157	434.8	328.20	135.6	96.8

the experimental data, most of which are out of the "small-q range". The obtained $\mathcal{R}_c(q = 0,T)$ and $\xi(T)$ are listed in Table IV. The relative errors due to employing the OZD equation could be up to 20% for both $\mathcal{R}_c(q = 0,T)$ and $\xi(T)$.

In the vicinity of the spinodal temperature the correlation length $\xi(T,\phi)$ is proportional to $|T - T_{sp}|^{-\nu}$.

$$\xi^{-1/\nu} \sim |T - T_{sp}|$$

from eq 29. The mean field assumption gives $\nu = {}^1/_2$; therefore

$$\xi^{-2} \sim |T - T_{sp}|$$

The spinodal temperature was obtained from the plot of $\xi^{-2}(T,\phi)$ vs. T, as shown in Figure 5. The obtained spinodal points were plotted as a function of ϕ in Figure 6 together with the cloud point, T_{cp}^N. The spinodal temperature is close to T_{cp}^N when $\phi \sim \phi_c$ and is far above it when $\phi \ll \phi_c$ or $\phi \gg \phi_c$, where ϕ_c is the volume fraction of the critical composition.

Critical Exponents. The concentration fluctuation of a polymer mixture is often discussed in terms of its critical exponents similar to the binary liquid case. Schelten et al.[18] obtained $\nu = 0.492 \pm 0.017$ and $\gamma = 0.997 \pm 0.085$ for

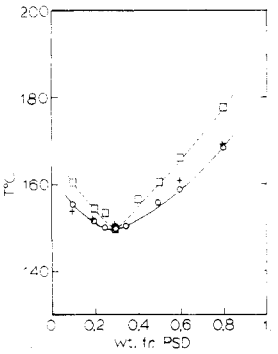

Figure 6. Phase diagram of PSD/PVME. The solid line with circles and the dashed line with squares show respectively the neutron cloud point (T_{cp}^{N}) curve and the spinodal curve (T_{sp}). The light cloud point (T_{cp}^{L}) is indicated by the crosses.

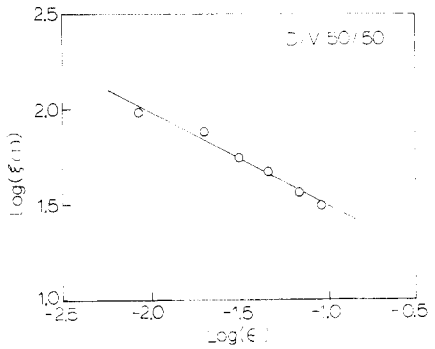

Figure 7. ϵ-Dependence of the correlation length ξ for D50.

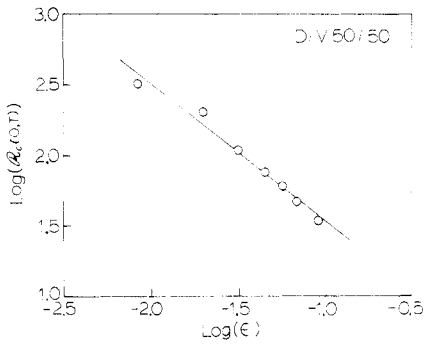

Figure 8. ϵ-Dependence of the Rayleigh factor at zero angle $\mathcal{R}_c(q = 0,T)$ for D50.

polystyrene–poly(vinyl methyl ether) blends, which are very close to the values of the mean field prediction (ν = 0.5 and γ = 1.0). Figures 7 and 8 show typical plots of log ξ vs. log ϵ and log $\mathcal{R}_c(0)$ vs. log ϵ for D50, which give ν = 0.49 ± 0.04 and γ = 0.98 ± 0.07. Experimental exponents for all compositions are listed in Table V, which support, again the validity of the mean field assumption.

Statistical Segment Length. From the nonlinear regression on eq 31 the average statistical segment length can be obtained as a function of composition and temperature by assuming Gaussian chain statistics as shown in Figure 9. Taking account of the experimental error, which would be up to ±0.5 Å, one can conclude there is only a very small dependence on temperature and no dependence on composition of the average statistical segment length $b(b \equiv (\overline{b^2})^{1/2})$. This negligible temperature dependence of b might result from the effects of the volume expansion and the shortening of the persistence length with temperature. The absolute value of b depends on v_0 and is 7.7 Å when v_0 = 74.7 cm^3/mol ($=(v_{PSD}v_{PVME})^{1/2}$).

One can get the statistical segment length for PS and PVME from the ratio between the root-mean-square

Table V
Critical Exponents

code	ν	ξ_0, Å	γ	$\mathcal{R}_{c0}(q = 0)$, cm^{-1}
D10	0.529 ± 0.16	17.9	1.06 ± 0.23	3.71
D20	0.504 ± 0.03	12.9	1.01 ± 0.06	3.53
D25	0.471 ± 0.04	13.6	0.94 ± 0.08	4.67
D30	0.595 ± 0.06	8.88	1.19 ± 0.12	2.30
D40	0.495 ± 0.04	11.5	0.99 ± 0.07	4.29
D50	0.490 ± 0.04	10.1	0.98 ± 0.07	3.60
D60	0.518 ± 0.01	8.76	1.04 ± 0.03	2.54
D80	0.518 + 0.02	9.85	1.03 ± 0.03	2.11

Table VI
Comparison of χ-Parameters of PS/PVME Obtained by SANS at Room Temperature

wt % PS (or PSD)	$\chi/v_0 \times 10^4$, mol/cm^3	$\chi \times 10^2$	remarks
10	−3.67	−2.74	this work
20	−3.21	−2.40	$v_0 = (v_{PSD}v_{PVME})^{1/2}$
25	−3.97	−2.96	
30	−4.01	−2.99	$M_{w,PSD}$ = 252 000
40	−4.05	−3.02	$M_{w,PVME}$ = 99 000
50	−4.93	−3.68	
60	−6.37	−4.75	
80	−4.90	−3.66	
75	−4.1		Hadziioannou et al.
50	−3.2		
<5		−4.0	Kirste et al.
<5	−1.85		$M_{w,PSD}$ = 25 000
<5	−1.24		$M_{w,PSD}$ = 63 000
<5	−1.45		$M_{w,PSD}$ = 188 000
<5	−0.93		$M_{w,PSD}$ = 465 000
			$M_{w,PVME}$ = 10 000, Jelenic et al.

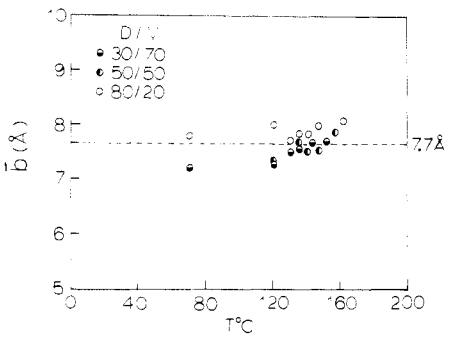

Figure 9. Temperature dependence of the statistical segment length $\bar{b}$ for various compositions. The dased line shows the average value 7.7 Å.

end-to-end distance $\langle r_0^2\rangle^{1/2}$ and the square root of the molecular weight, $c = \langle r_0^2\rangle^{1/2}/M^{1/2}$. b_i is given by

$$b_i = c_i m_i^{1/2}$$

where m_i is again the monomer molecular weight. c_{PSH} and c_{PVME} are respectively 0.67 ± 0.015 and 0.9 ± 0.05 Å,[30] thus giving b_{PSD} = 6.8 Å and b_{PVME} = 6.9 Å. We assumed here $b_{PSD} = b_{PSH}$, where PSH denotes hydrogenated polystyrene. Substituting these numbers and the heterogeneity index of molecular weight, $\langle M_i\rangle_z/\langle M_i\rangle_w$, into eq 24, one gets the average statistical segment length b, which is 8.5 Å and is only slightly larger than the experimental result. This agreement shows not only the validity of Joanny's theory on polydispersity but also the accuracy of the experiments.

χ-Parameter Analysis. Table VI shows the χ-parameters of PS/PVME at room temperature (around 25 °C) obtained by several workers by means of the SANS technique. There are two definitions of χ, the χ per unit volume χ/v_0 and that per lattice volume χ. Jelenic et al.[8] chose dilute systems and used the Zimm equation to evaluate χ, and they found a molecular weight dependence

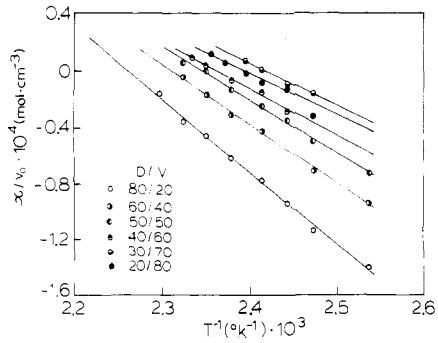

Figure 10. Reciprocal temperature dependence of χ/v_0 for various compositions.

for χ. Hadziioannou et al.[31a] proposed a method to obtain χ by modifying the Zimm equation to a ternary system in which two components are isotopes with the same molecular length and then obtained χ[31b] that is close to the results obtained by a vapor pressure measurement. All experimental values of χ and/or χ/v_0 are in good agreement in magnitude. These data show the systematic variation of χ with composition and molecular weight.

Figure 10 shows the reciprocal temperature dependence of χ/v_0 for all compositions. This shows that the χ/v_0 depends not only on temperature but also on composition. In the context of the Flory–Huggins lattice theory, χ is independent of composition. Therefore, we have to employ a more general theory to account for these experimental results that show a composition dependence of χ, actually the composition dependence of the "apparent χ."

Either Flory and Patterson's equation of state theory[13,14] or Sanchez's lattice fluid theory[15,16] might be applied to this problem. Schmitt et al.[8] used the Flory–Patterson theory and obtained the enthalpic and entropic parameters X_{12} and Q_{12}, respectively, and a general form of χ as a function of temperature for several kinds of polymer blends, including PS/PVME.

We utilize here the Sanchez lattice fluid theory[15,16] because of the more general treatment and the explicit expressions for the chemical potential and the spinodal criteria. The free energy per mole of unit cell of a lattice fluid composed of two components is given by

$$\Delta G_{LF} = E^*\left\{-\tilde{\rho} + \tilde{P}\tilde{v} + \tilde{T}\left[(\tilde{v}-1)\ln(1-\tilde{\rho}) + \left(\frac{\phi_A}{y_A} + \frac{\phi_B}{y_B}\right)\ln\tilde{\rho} + \frac{\phi_A}{y_A}\ln\left(\frac{\phi_A}{\omega_A}\right) + \frac{\phi_B}{y_B}\ln\left(\frac{\phi_B}{\omega_B}\right)\right]\right\} \quad (34)$$

where $\tilde{\rho}$, $\tilde{P}$, $\tilde{v}$, and $\tilde{T}$ are respectively the reduced variables for the density, pressure, volume, and temperature with respect to the corresponding characteristic quantities ρ^*, P^*, v^*, and T^*. ω_i is the coordination number of the fluid lattice. E^* is the cell interaction energy and is given by

$$E^* = \sum_i\sum_j E^*_{ij} = \sum_i \phi_i E^*_{ij} - RT\sum_i\sum_j \phi_i\phi_j\chi_0 \qquad i,j = A, B$$

and

$$\chi_0 \equiv (E^*_{AA} + E^*_{BB} - 2E^*_{AB})/RT \quad (35)$$

The second derivative of eq 34 gives the criteria of the spinodal and the Rayleigh factor at zero angle as we discussed in section II, which is

$$\frac{1}{RT}\frac{\partial^2}{\partial\phi_A{}^2}\Delta G_{LF} = \frac{k_N v_0}{\mathcal{R}_c(0,T)} = \frac{1}{\phi_A y_A} + \frac{1}{\phi_B y_B} - \tilde{\rho}(2\chi_0 + \tilde{T}\psi^2 P^*\beta) \quad (36)$$

where

$$\psi = \tilde{\rho}\left[\frac{1}{\tilde{T}_A} - \frac{1}{\tilde{T}_B} + (\phi_A - \phi_B)\chi_0\right] - \left(\frac{1}{y_A} - \frac{1}{y_B}\right)$$

and β is the isothermal compressibility of the mixture and is

$$\beta = \frac{\partial \ln \tilde{v}}{\partial P}\bigg|_T$$

therefore

$$\frac{k_N}{\mathcal{R}_c(0,T)} = \frac{1}{v_0}\left[\frac{1}{\phi_A y_A} + \frac{1}{\phi_B y_B} - \tilde{\rho}(2\chi_0 + \tilde{T}\psi^2 P^*\beta)\right] = \frac{1}{\phi_A v_A z_A} + \frac{1}{\phi_B v_B z_B} - \tilde{\rho}\left(\frac{2\chi_0}{v_0} + \frac{\tilde{T}\psi^2 P^*\beta}{v_0}\right) \quad (37)$$

When $\beta = 0$, $\tilde{\rho} = 1$, and eq 36 is reduced to eq A-3 or A-5, which is the incompressible limit treated by Flory and Huggins.

When $\beta \neq 0$, one has to worry about the functional form of the right-hand side of eq 37. Let us redefine χ as

$$\chi = \tfrac{1}{2}\tilde{\rho}(2\chi_0 + \tilde{T}\psi^2 P^*\beta) \quad (38)$$

Assuming no temperature dependence of E^*_{ij} $(i, j = A, B)$, one can obtain

$$\chi_0 = \Lambda/T \quad (39)$$

where Λ is a constant. Substituting eq 39 into eq 38, one finally gets the equation

$$\frac{\chi}{v_0} = \frac{1}{Tv_0}\left\{\tilde{\rho}\Lambda + \frac{\tilde{\rho}^3}{2T^*}[(T^*_A - T^*_B) + (\phi_A - \phi_B)\Lambda]^2 P^*\beta\right\} - \frac{1}{v_0}\left\{\frac{\tilde{\rho}^2}{T^*}P^*\beta[(T^*_A - T^*_B) + (\phi_A - \phi_B)\Lambda]\left(\frac{1}{y_A} - \frac{1}{y_B}\right)\right\} + \frac{T}{v_0}\left\{\frac{\tilde{\rho}}{2T^*}\left(\frac{1}{y_A} - \frac{1}{y_B}\right)^2 P^*\beta\right\} \quad (40)$$

In the case of polymeric mixtures, one can neglect the second and third terms of the right-hand side of eq 40 because

$((1/y_A) - (1/y_B)) \ll 1$, so

$$\frac{\chi}{v_0} \cong \frac{1}{Tv_0}\left\{\tilde{\rho}\Lambda + \frac{\tilde{\rho}^3}{2T^*}[(T^*_A - T^*_B) + (\phi_A - \phi_B)\Lambda]^2 P^*\beta\right\} \quad (41)$$

Both the reduced density $\tilde{\rho}$ and the compressibility β may have temperature and composition dependence. The reduced density $\tilde{\rho}$ may be written as

$$\tilde{\rho} \equiv \frac{1}{\tilde{v}} = [1 + \alpha(\phi)T]^{-1} \cong 1 - \alpha(\phi)T \quad (42)$$

and the compressibility β as

$$\beta = Be^{bT} \quad (43)$$

then eq 41 reduces to

$$\frac{\chi}{v_0} = \frac{1}{Tv_0}\left\{(1 - \alpha T)\Lambda + \frac{1 - 3\alpha T}{2T^*}[(T^*_A - T^*_B) + (\phi_A - \phi_B)\Lambda]^2 P^* B e^{bT}\right\} \quad (44)$$

Equation 44 shows that χ/v_0 is a nonlinear function of

temperature and composition. We feel that a direct fitting of current χ/v_0 data to eq 44 as a function of α and β (or an approximated form as a function of T and ϕ) could lead to erroneous or at least inaccurate results. Further analysis of χ/v_0 may be pursued when more detailed results of χ/v_0, α, and β are available.

Conclusion

The "neutron" cloud points observed by the temperature-scanning small-angle neutron scattering technique are in good agreement with the "light" cloud point. This fact means that the growth of the concentration fluctuations is fast enough[26] compared with the heating rate of the experiments so that there is a negligible kinetic effect in the cloud point measurements.

With the use of the de Gennes scattering function for blends, the correlation length, the statistical segment length, and the χ-parameter were obtained as functions of temperature and composition. The observed statistical segment length was 7.7 Å, which is in good agreement with the calculated value, 8.5 Å, taking account of polydispersity. The spinodal temperature, which was obtained by the correlation length extrapolation, is above the cloud point curve as expected for LCST systems. The critical exponents ν and γ were around 0.5 and 1.0, respectively, which means the system can be described by mean field theory.[24]

A composition dependence for χ was observed and compared qualitatively to the Sanchez fluid lattice theory. The χ-parameter may be written as

$$\chi = \chi(\phi,T) = \chi_1(\phi,T)/T + \chi_2(\phi,T)$$

The composition dependence of χ may be due to both thermal expansion and compressibility of the fluid lattice nature of the blends.

Acknowledgment. We thank Drs. I. C. Sanchez, C. Glinka, and M. Okada, National Bureau of Standards, for fruitful discussions and their help in the SANS experiments. The University of Massachusetts group acknowledges financial support from the Division of Material Research, National Science Foundation, the Army Research Office (Durham), the Material Research Laboratory of the University of Massachusetts, and Xerox Corp.

Appendix

Modified Zimm Equations. From eq 15 and the relationship

$$\mathcal{R}_c = k_N \frac{RT\phi_B}{\partial\Delta\mu_A/(\partial\phi_A)} \tag{A-1}$$

where $\Delta\mu_A$ is the chemical potential of A, we obtain

$$\Delta\mu_A = -RT[\ln\phi_A + (1 - (y_A/y_B))\phi_B + y_A\chi\phi_B^2] \tag{A-2}$$

Combining eq A-2 with eq 3, we obtain eq 16 and 17 in the text. We call eq 17 the modified Zimm equation to distinguish from eq 12. Equation 16 can also be written as

$$\frac{1}{\mathcal{R}_c(0,T)}N\left(\frac{a_A}{v_A} - \frac{a_B}{v_B}\right)^2 = \frac{1}{v_0}\left[\frac{1}{y_A\phi_A} + \frac{1}{y_B\phi_B}\right] - \frac{2\chi}{v_0} \tag{A-3}$$

$$\frac{1}{\mathcal{R}_c(0,T)}N\left(\frac{a_A}{v_A} - \frac{a_B}{v_B}\right)^2 = \frac{1}{v_A z_A\phi_A} + \frac{1}{v_B z_B\phi_B} - \frac{2\chi}{v_0} \tag{A-4}$$

In terms of eq 10 and the definition of the spinodal point

$$\frac{1}{RT}\left(\frac{\partial^2\Delta G}{\partial\phi_i^2}\right) = \frac{1}{v_A z_A\phi_A} + \frac{1}{v_B z_B\phi_B} - \frac{2\chi_s}{v_0} = 0 \tag{A-5}$$

Equations A-3 and A-4 are rewritten as

$$\frac{k_N}{\mathcal{R}_c(0,T)} = \frac{2}{v_0}(\chi_s - \chi) \tag{A-6}$$

where χ_s is the Flory–Huggins interaction parameter at the spinodal, and

$$\chi_s = \frac{1}{2}\left[\frac{1}{y_A\phi_A} + \frac{1}{y_B\phi_B}\right] = \frac{v_0}{2}\left[\frac{1}{v_A z_A\phi_A} + \frac{1}{v_B z_B\phi_B}\right] \tag{A-7}$$

Equations 16, 17, A-3, A-4, and A-6 are identical and allow us to estimate the χ-parameter for any composition.

de Gennes Scattering Function. We will review the de Gennes scattering function with emphasis on the inequality of the segment volumes:

The local compositional fluctuation of A at $\mathbf{r}$, $\delta\phi_A(\mathbf{r})$ is given by

$$\delta\phi_A(\mathbf{r}) = (1/V)\left\langle \int d\mathbf{r}' \sum_t^{N_A}\sum_{j_t}^{z_A}\xi_{i_s i_t}(\mathbf{r} - \mathbf{r}')W_{j_t}(\mathbf{r}')\right\rangle_{i_s,s} \tag{A-8}$$

where $\xi_{i_s j_t}(\mathbf{r} - \mathbf{r}')$ is the response function of ith segment on the sth chain and the jth segment on the tth chain at $\mathbf{r}'$, $W_{j_t}(\mathbf{r}')$ being the reduced external potential applied on the j_tth segment. $\langle\ \rangle_{i_s,s}$ denotes to take an ensemble average with respect to the chain s and the segment i_s. N_A and V are the number of A chains in the system and the volume of the system, respectively. Here we assumed monodispersity of the components; i.e., each A chain has the polymerization index of z_A. Equation A-8 is written as

$$\delta\phi_A(\mathbf{r}) = (1/N_A V)\sum_s^{N_A}(1/z_A)\sum_{i_s}^{z_A}\int d\mathbf{r}' \sum_t^{N_A}\sum_{j_t}^{z_A}\xi_{i_s j_t}(\mathbf{r} - \mathbf{r}')W_{j_t}(\mathbf{r}') \tag{A-9}$$

In the Fourier space eq A-8 is given by

$$\delta\tilde{\phi}_A(\mathbf{q}) = (\phi_A/N_A)\sum_s^{N_A}(1/z_A)\sum_{i_s}^{z_A}\sum_t^{N_A}\sum_{j_t}^{z_A}\tilde{\xi}_{i_s j_t}(\mathbf{q})\tilde{W}_{j_t}(\mathbf{q}) \tag{A-10}$$

where $\tilde{\phi}_A(\mathbf{q})$ denotes the Fourier conjugate of $\tilde{\phi}_A(\mathbf{r})$ at the average composition, at ϕ_A, and results from the integration over the volume elements of the A segments. In the context of the mean field approximation, each A segment feels the same potential, $\tilde{W}_A(\mathbf{q})$ independent of j and t

$$\delta\tilde{\phi}_A(\mathbf{q}) = [(\phi_A/N_A)\sum_s^{N_A}(1/z_A)\sum_{i_s}^{z_A}\sum_t^{N_A}\sum_{j_t}^{z_A}\tilde{\xi}_{i_s j_t}(\mathbf{q})]\tilde{W}_A(\mathbf{q}) \tag{A-11a}$$

Equation A-11a can be divided into two parts

$$\delta\tilde{\phi}(\mathbf{q}) = (\phi_A/N_A)\sum_s^{N_A}(1/z_A)[\sum_{i_s}^{z_A}\sum_{j_s}^{z_A}\tilde{\xi}_{i_s j_s}(\mathbf{q})\tilde{W}_A(\mathbf{q}) + \sum_{i_s}^{z_A}\sum_{t\neq s}^{N_A}\sum_{j_t}^{z_A}\tilde{\xi}_{i_s j_t}(\mathbf{q})\tilde{W}_A(\mathbf{q})] \tag{A-11b}$$

The first and the second terms of the right-hand side of eq A-11b mean, respectively, the contribution of the intra- and interchain interactions. Equation A-11b is also given in terms of the correlation function, $S_A(\mathbf{q})$

$$\delta\tilde{\phi}_A(\mathbf{q}) = \tilde{S}_A(\mathbf{q})\tilde{W}_A(\mathbf{q}) = [\tilde{S}_A{}^{\circ}(\mathbf{q}) + \delta\tilde{S}_A(\mathbf{q})]\tilde{W}_A(\mathbf{q}) \tag{A-12}$$

where

$$\tilde{S}_A(\mathbf{q}) = (\phi_A/N_A)\sum_s^{N_A}(1/z_A)\sum_{i_s}^{z_A}\sum_t^{N_A}\sum_{j_t}^{z_A}\tilde{\xi}_{i_s j_t}(\mathbf{q}) \tag{A-13a}$$

and

$$\tilde{S}_A^\circ(\mathbf{q}) = (\phi_A/N_A)\sum_s^{N_A}(1/z_A)\sum_{i_s}^{z_A}\sum_{j_s}^{z_A}\tilde{\xi}_{i_sj_s}(\mathbf{q}) \quad \text{(A-13b)}$$

$S_A^\circ(\mathbf{q})$ is called as the "bare" correlation function and no interchain interactions are involved. In this case $\tilde{\xi}_{i_sj_s}(\mathbf{q})$ has already been obtained as

$$\tilde{\xi}_{i_sj_s}(\mathbf{q}) = \exp[-|i_s - j_s|b_K^2q^2/6] \quad \text{(A-14)}$$

and $\tilde{S}^\circ_A(\mathbf{q})$ is given in terms of the Debye function, $g_D(u_K)$, as follows[22]

$$\tilde{S}_A^\circ(\mathbf{q}) = \phi_A(v_0/v_A)z_Ag_D(u_K) \quad \text{(A-15)}$$

$$g_D(u_K) = (2/u_K^2)(e^{-u_K} - 1 + u_K) \quad \text{(A-16a)}$$

$$u_K = q^2R_{gK}^2 = (z_Kb_K^2/6)q^2 \quad \text{(A-16b)}$$

where b_K and R_{gK} are the statistical segment length and the radius of gyration of the K-kind chain.

In the case where the interaction potential between A and B monomers is nonzero, with the linear response assumption, eq A-12 is rewritten as follows

$$\delta\tilde{\phi}_A(\mathbf{q}) = \tilde{S}_A(\mathbf{q})\tilde{W}_A(\mathbf{q}) = \tilde{S}_A^\circ(\mathbf{q})[\tilde{W}_A(\mathbf{q}) - U\delta\tilde{\phi}_B(\mathbf{q}) + v_A\delta\tilde{\Omega}(\mathbf{q})] \quad \text{(A-17a)}$$

where U and $\delta\tilde{\Omega}(\mathbf{q})$ are respectively the interaction parameter and the Lagrange multiplier. Similarly, for the B chain

$$\delta\tilde{\phi}_B(\mathbf{q}) = \tilde{S}_B(\mathbf{q})\tilde{W}_B(\mathbf{q}) = \tilde{S}_B^\circ(\mathbf{q})[\tilde{W}_B(\mathbf{q}) - U\delta\tilde{\phi}_A(\mathbf{q}) + v_B\delta\tilde{\Omega}(\mathbf{q})] \quad \text{(A-17b)}$$

Applying the incompressibility of the system

$$v_A\delta\tilde{\phi}_A(\mathbf{q}) + v_B\delta\tilde{\phi}_B(\mathbf{q}) = 0 \quad \text{(A-18)}$$

one can solve $(\delta\tilde{\phi}_A, \delta\tilde{\phi}_B)$ as a function of $(\tilde{W}_A, \tilde{W}_B)$. The solution is

$$(\delta\tilde{\phi}_A, \delta\tilde{\phi}_B) = \mathbf{s}\begin{pmatrix}\tilde{W}_A\\ \tilde{W}_B\end{pmatrix} \quad \text{(A-19)}$$

$$\mathbf{S} = \frac{S_A^\circ S_B^\circ}{S_A^\circ v_A^2 - 2US_A^\circ S_B^\circ v_Av_B + S_B^\circ v_B^2}\times \begin{pmatrix} v_B^2 & -v_Av_B\\ -v_Av_B & -v_A^2\end{pmatrix} \quad \text{(A-20)}$$

The scattering intensity per mole of unit cell is given by

$$I(q) = (a_A, a_B)\mathbf{S}\begin{pmatrix}a_A\\ a_B\end{pmatrix} = (v_Ba_A - v_Aa_B)^2 \times \frac{S_A^\circ(q)\,S_B^\circ(q)}{v_A^2S_A^\circ(q) - 2Uv_Av_BS_A^\circ(q)S_B^\circ(q) + v_B^2S_B^\circ(q)} \quad \text{(A-21)}$$

knowing

$$I(q) = v_0R_c(q) \quad \text{(A-22)}$$

and using eq 10, one obtains eq 18 and 19 in the text.

Registry No. PVME (homopolymer), 9003-09-2; polystyrene (homopolymer), 9003-53-6; neutron, 12586-31-1.

References and Notes

(1) See, for example: Paul, D. R., Newman, S., Eds., "Polymer Blends"; Academic Press: New York, 1978.
(2) See, for example: Russell, T. P.; Stein, R. S. *J. Macromol. Sci., Phys.* **1980** *B17* (4), 617.
(3) de Gennes, P.-G. "Scaling Concepts in Polymer Physics"; Cornell University Press: New York, 1979; Chapter IV.
(4) Hadziioannou, G.; Gilmer, J.; Stein, R. S. *Polym. Bull. (Berlin)* **1983**, *9*, 563. Stein, R. S.; Hadziioannou, G. *Macromolecules* **1984**, *17*, 1059
(5) Walner, M.; Higgins, J. S.; Carter, A. J. *Macromolecules* **1983**, *16*, 1931.
(6) Benoit, H.; Benmouna, M., submitted to *Polymer*.
(7) Benoit, H.; Benmouna, M. *Macromolecules* **1984**, *17*, 535.
(8) Jelenic, J.; Kirste, R. G.; Oberthur, R. C.; Schmitt-Strecker, S.; Schmitt, B. J. *Makromol. Chem.* **1984**, *185*, 129.
(9) Murray, C. T.; Gilmer, J. W.; Stein, R. S. *Macromolecules* **1985**, *18*, 996.
(10) Gee, G.; Orr, W. J. C. *Trans. Faraday Soc.* **1946**, *42*, 507. Bawn, C. E. H.; Freeman, R. F. J.; Kamaliddin, A. R. *Trans. Faraday Soc.* **1950**, *46*, 677. Newing, M. J. *Trans. Faraday Soc.* **1950**, *46*, 613.
(11) Koningsveld, R.; Kleintjens, L. A.; Schultz, A. R. *J. Polym Sci., Part A-2* **1970**, *8*, 1261.
(12) Koningsveld, R.; Kleintjens, L. A. *J. Polym. Sci., Polym. Symp.* **1977**, *61*, 211. Roe, R. J.; Zin, W. C. *Macromolecules* **1980**, *13*, 1221.
(13) Flory, P. J.; Orwall, R. A.; Vrij, A. *J. Am. Chem. Soc.* **1964**, *86*, 3507.
(14) Patterson, D.; Bhattacharyya, S. N.; Picker, P. *Trans. Faraday Soc.* **1968**, *64*, 648.
(15) Sanchez, I.C.; Lacombe, R. H. *J. Phys. Chem.* **1976**, *80*, 2352.
(16) Lacombe, R. H.; Sanchez, I. C. *J. Phys. Chem.* **1976**, *80*, 2568.
(17) Yang, H.; Shibayama, M.; Stein, R. S.; Han, C. C. *Polym. Bull. (Berlin)* **1984**, *12*, 7.
(18) Herkt-Maetzky, C.; Schelten, J. *Phys. Rev. Lett.* **1983**, *51*, 896.
(19) Joanny, J. F. *C. R. Sceances Acad. Sci., Ser. B* **1978**, *286*, 89.
(20) Einstein, A. *Ann. Phys. (Leipzig)* **1910**, *33*, 1275.
(21) Debye, P. *Appl. Phys.* **1944**, *15*, 338.
(22) In ref 5 the authors did not take into account the correction of the difference of the segment volume. Due to the identity $\tilde{S}_A^\circ(q)v_A = \phi_Az_Av_Ag_D(u_A) = \phi_Ay_Av_0g_D(u_A)$, $(\tilde{S}_A^\circ(q) = \phi_A(v_0/v_A)z_Ag_D(u_A)$ (eq A-15); similarly, $U = (v_Av_B/v_0^2)\chi$.
(23) Brinkman, H. C.; Hermans, J. J. *J. Chem. Phys.* **1949**, *17*, 574.
(24) See, for example: Stanley, H. E. "Introduction to Phase Transitions and Critical Phenomena"; Oxford University Press: New York, 1971.
(25) Glinka, C., private communication, National Bureau of Standards.
(26) Yang, H.; Shibayama, M.; Stein, R. S.; Shimizu, N.; Hashimoto, T., to be submitted.
(27) Hashimoto, T.; Kumaki, J.; Kawai, H. *Macromolecules* **1983**, *16*, 641.
(28) Nishi, T.; Wang, T. T.; Kwei, H. *Macromolecules* **1975**, *8*, 227.
(29) Reich, S.; Cohen, Y. *J. Polym. Sci., Polym. Phys. Ed.* **1981**, *19*, 1255.
(30) Brandrup, J., Immergut, E. H., Eds. "Polymer Handbook"; Wiley: New York, 1975.
(31) (a) Hadziioannou, G.; Stein, R. S. *Macromolecules* **1984**, *17*, 567. (b) The definition of χ in ref 31a is changed between the Theoretical Section and the Experimental Section. The χ listed in tables in ref 31a is the interaction parameters per unit volume, not per lattice, which corresponds to χ/v_0 in this paper.
(32) Certain commercial equipment, instruments, or materials are identified in this paper in order to adequately specify the experimental procedure. Such identification does not imply recommendation or endorsement by the National Bureau of Standards nor does it imply that the materials or equipment identified are necessarily the best available for the purpose.